Spin-wave analysis of the sublattice magnetization of the quadratic double-layer antiferromagnet $K_3Mn_2F_7$

A. F. M. Arts and H. W. de Wijn
Fysisch Laboratorium, Rijksuniversiteit, Utrecht, The Netherlands
(Received 15 November 1976)

The variation with temperature of the sublattice magnetization of the quadratic double-layer antiferromagnet $K_3Mn_2F_7$ has been determined by measuring the NMR frequency of the ^{19}F nuclei adjacent to the Mn sites in the double layer. The data have been analyzed in terms of a two-dimensional four-sublattice spin-wave theory. Temperature-dependent and temperature-independent renormalization as formulated by Oguchi, as well as temperature variation of the $k = 0$ energy gap have been included, while the integrations over the Brillouin zone have been carried out exactly. The dispersion is 2×2 fold degenerate, where the lower branches represent in-phase and the upper branches, with energy larger than $4|J|S$, out-of-phase precession of the spins in the paired layers, respectively. In a least-squares adjustment, spin-wave theory then appears to account for the sublattice magnetization up to 28 K, to be compared with $T_N = 58$ K. The least-squares adjustment yielded for the exchange constant $J/k_B = -7.59 \pm 0.03$ K and for the zero-temperature energy gap $T_G(0) = 5.99 \pm 0.06$ K (including effects of residual c-axis dispersion), which corresponds to an anisotropy field $H_A = 1.4$ kG. In contrast to the single-layer structure K_2MnF_4, Oguchi renormalization resulted in a marked improvement, by 9 K, of the range of concurrence over the unrenormalized theory. The functional dependence of the sublattice magnetization of $K_3Mn_2F_7$ on temperature is found to be close to that in the single-layer K_2MnF_4, at least at such low temperatures, that the upper magnon branches are not yet excited. Finally, evidence is found for zero-point spin reduction in good accord with the spin-wave value $\Delta_0 = 0.124$.

I. INTRODUCTION

During the last few years there has been a great deal of interest in the magnetic properties of lower-dimensional antiferromagnets,[1] in particular the quadratic-layer structures with crystallographic formula K_2MnF_4. The magnetic ions of these systems are situated in layers consisting of a simple-quadratic lattice, with a nearest-neighbor exchange at least several orders of magnitude stronger than the interaction between the layers. Further, in virtue of the staggered registry of adjacent layers the exchange interactions between them cancel, and indeed the members of the K_2MnF_4 family have proved to be very good examples of two-dimensional (2D) antiferromagnetic ordering.[2-4]

In this paper, we present an analysis of the temperature dependence of the sublattice magnetization, as reflected in the NMR frequency of ^{19}F nuclei, in $K_3Mn_2F_7$, a structure expected to be magnetically intermediate to K_2MnF_4 and the three-dimensional (3D) antiferromagnet $KMnF_3$. The crystallographic structure of $K_3Mn_2F_7$ closely resembles the single-layer structure K_2MnF_4 in the sense that Mn-F layers are substituted by sheets of unit cells of the perovskite $KMnF_3$ (Fig. 1). Magnetically, the lattice of $K_3Mn_2F_7$ consists of sheets of two adjoining layers of antiferromagnetically ordered Mn^{2+} spins. Each spin is surrounded by five nearest Mn^{2+} neighbors, one of which is located in the adjoining layer. By the same argument as in K_2MnF_4, i.e., every exchange path to a Mn^{2+} spin in an adjacent double layer is cancelled by a path to a spin with opposite sign, there is no net interaction between two adjacent double layers, at least not for $k = 0$ spin waves. There may exist some residual exchange between next-nearest double layers, but because of the large distance, involving many intermediate ions, this interaction is expected to be orders of magnitude weaker than the exchange within the paired layers. The magnetic double-layer character of this type of structure has recently been established by Gurewitz *et al.*[5] in a neutron-scattering experiment on the isomorph $Rb_3Mn_2Cl_7$ below the ordering temperature. Rods of reflection were observed, which in themselves are distinctive for a layer structure. The double-layer character was evidenced by the intensity modulation of the rods with a wave vector $2\pi/a'$, where a' is the intrapair distance between the layers. In the isomorphic compound $K_3Ni_2F_7$ Raman scattering has earlier been reported by Ferguson *et al.*,[6] while the optical properties were investigated by Pisarev *et al.*[7]

A principal point of interest is of course the question whether the double layer will show the characteristics of the 2D systems or rather resembles the 3D structures. Here one should distinguish between on one hand thermodynamic quantities that reflect the short-range order, such as the susceptibility and the specific heat, and on the other hand the sublattice magnetization, which is

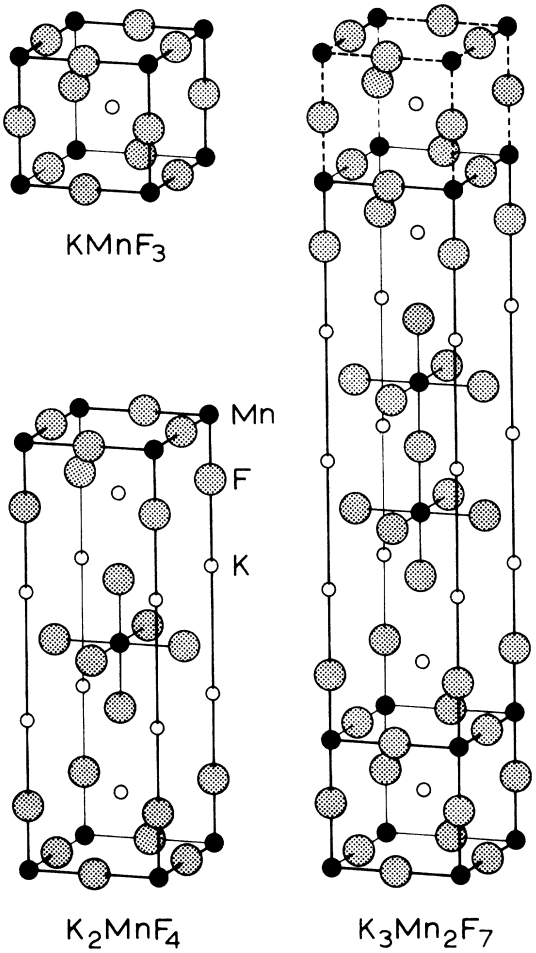

FIG. 1. Crystallographic unit cell of $K_3Mn_2F_7$, as compared to those of $KMnF_3$ and K_2MnF_4. The cell of $K_3Mn_2F_7$ has been extended along the tetragonal axis to indicate more clearly the magnetic double-layer structure.

predominantly determined by long-range correlations. It has been worked out[8] that in thin magnetic films only four layers have to be stacked for a virtually 3D behavior of the susceptibility and the specific heat. The amount of short-range order is reflected in the area of the broad maximum in the susceptibility just above T_N. The maximum found to occur in the 2D structures appears to be more pronounced than in the 3D case.[2] For the double layer the calculations indicate a substantial reduction of the maximum relative to 2D, in the direction of 3D, which indeed has been observed.[9,10] For the sublattice magnetization the situation is different in the sense that the temperature dependence is mainly determined by long-range correlations, extending over distances much longer than the lattice parameter. In the direction perpendicular to the double layer, long-range order cannot be sustained, so that the functional dependence of the magnetization on temperature is expected to be close to that in the 2D single-layer structure.

Spin-wave theory is acknowledged to describe the sublattice magnetization up to some temperature below T_N. In three dimensions, Low[11] successfully fit the sublattice magnetization in MnF_2 up to as high as $0.9T_N$, where the magnetization has already dropped to 50% of the value at $T=0$ K. Temperature-dependent spin-wave renormalization, as was first formulated by Oguchi,[12] was included in his calculation. In the 2D case, the results of spin-wave theory appeared to be less impressive. de Wijn, Walker, and Walstedt[4] measured the sublattice magnetization of the almost ideal 2D compounds K_2NiF_4, K_2MnF_4, and Rb_2MnF_4, and found excellent agreement between experiment and renormalized theory up to a temperature slightly below $\frac{1}{2}T_N$. At the point of failure of spin-wave theory, the thermal deviation from complete alignment in K_2NiF_4 is only 4%, added to 18% zero-point motion. For K_2MnF_4 and Rb_2MnF_4 the failure occurs at 7% thermal motion, while the zero-point spin reduction is also 7%. Temperature-dependent spin-wave renormalization did not essentially improve the fit in K_2NiF_4, and a marginal improvement by 3 K was obtained in the Mn compounds. Temperature-independent renormalization, however, results in an essential modification of the spin-wave parameters, such as the exchange constant. In 2D, excitations which cannot be properly described in terms of spin waves apparently extend over a much larger temperature region below the transition point than is the case in 3D. Accordingly, one objective of the following analysis is to see what improvement can be obtained by including renormalization in the double layer, in which each magnetic ion is surrounded by five instead of four nearest neighbors and the spatial coherence of the lattice is correspondingly increased.

II. SPIN-WAVE THEORY

In this section, we develop a two-dimensional four-sublattice spin-wave theory with inclusion of renormalization, as pertinent to the simple-quadratic double-layer antiferromagnet, and review the general features of the dispersion relation, the sublattice magnetization, and zero-point spin reduction in some detail. The method of applying the results of this section to $K_3Mn_2F_7$ (Sec. IV) closely resembles the earlier analysis of K_2MnF_4 and isomorphs by de Wijn, Walker, and Walstedt,[4] and one is referred to this reference for further

details on the assumptions on which the interpretation is based.

To analyze the data we have used a model with isotropic antiferromagnetic exchange J between nearest neighbors and a temperature-dependent staggered anisotropy field H_A in the direction of the tetragonal axis. In zero magnetic field the Hamiltonian may then be written

$$\begin{aligned}\mathcal{H} = {} & |J| \sum_{\langle l,m\rangle} \vec{S}_l \cdot \vec{S}_m + |J| \sum_{\langle l',m'\rangle} \vec{S}_{l'} \cdot \vec{S}_{m'} \\ & + |J| \sum_{\langle l,m'\rangle} \vec{S}_l \cdot \vec{S}_{m'} + |J| \sum_{\langle l',m\rangle} \vec{S}_{l'} \cdot \vec{S}_m \\ & - g\mu_B H_A \Big(\sum_l S_l^z - \sum_m S_m^z + \sum_{l'} S_{l'}^z - \sum_{m'} S_{m'}^z \Big) ,\end{aligned} \tag{1}$$

with the usual notation ($g = g_e$). The summations over the magnetic ions are split up over four sublattices, two of them located in the lower layer with indices l (spin up) and m (spin down), and two located in the upper layer with indices l' (spin up) and m' (spin down). The registry of l' and m' with respect to l and m is such that the l and m' sublattices, and similarly the l' and m sublattices, are adjacent to each other. Following the standard approach,[13] we proceed by going over to local spin-deviation operators through the Holstein-Primakoff transformations

$$\begin{aligned} & S_l^+ = (2S)^{1/2} f_l a_l , \quad S_m^+ = (2S)^{1/2} b_m^\dagger f_m , \\ & S_l^- = (2S)^{1/2} a_l^\dagger f_l , \quad S_m^- = (2S)^{1/2} f_m b_m , \\ & S_l^z = S - a_l^\dagger a_l , \quad S_m^z = -S + b_m^\dagger b_m , \end{aligned} \tag{2}$$

with

$$f_l = (1 - a_l^\dagger a_l / 2S)^{1/2} , \quad f_m = (1 - b_m^\dagger b_m / 2S)^{1/2}$$

(similarly for the primed sublattices with magnon operators $c_{l'}$ and $d_{m'}$), and introducing spatial Fourier transforms $a_{\vec{k}}$, $b_{\vec{k}}$, $c_{\vec{k}}$, and $d_{\vec{k}}$ over the sublattices l, m, l', and m', respectively.

In order to demonstrate the general features of the dispersion relation we first discuss the *un*renormalized theory, i.e., terms of order $1/2S$ and higher are neglected. At low temperatures this will generally be invisible in the temperature dependence of the sublattice magnetization as compared to the renormalized theory, except for the replacement of J by an effective exchange interaction J_s and an effective spin-wave energy gap,[4] to which we return later. We then find

$$\begin{aligned}\mathcal{H} = {} & C + (g\mu_B H_A + 5|J|S) \\ & \times \sum_{\vec{k}} (a_{\vec{k}}^\dagger a_{\vec{k}} + b_{\vec{k}}^\dagger b_{\vec{k}} + c_{\vec{k}}^\dagger c_{\vec{k}} + d_{\vec{k}}^\dagger d_{\vec{k}}) \\ & + 4|J|S \sum_{\vec{k}} \gamma_{\vec{k}} (a_{\vec{k}} b_{\vec{k}} + c_{\vec{k}} d_{\vec{k}} + a_{\vec{k}}^\dagger b_{\vec{k}}^\dagger + c_{\vec{k}}^\dagger d_{\vec{k}}^\dagger) \\ & + |J|S \sum_{\vec{k}} (a_{\vec{k}} d_{\vec{k}} + b_{\vec{k}} c_{\vec{k}} + a_{\vec{k}}^\dagger d_{\vec{k}}^\dagger + b_{\vec{k}}^\dagger c_{\vec{k}}^\dagger) ,\end{aligned} \tag{3}$$

with $C = -10|J|N_0 S^2 - 4g\mu_B N_0 S H_A$, and where N_0 is the number of magnetic ions in a particular sublattice. The summations run over a 2D square Brillouin zone, while $\gamma_{\vec{k}}$ is a geometrical factor given by

$$\gamma_{\vec{k}} = \frac{1}{4} \sum_{\vec{\delta}} e^{i\vec{k}\cdot\vec{\delta}} = \cos(\tfrac{1}{2} k_x a) \cos(\tfrac{1}{2} k_y a) , \tag{4}$$

with $\vec{\delta}$ a nearest-neighbor displacement within one of the paired layers, and a the dimension of the 2D magnetic unit cell.

The Hamiltonian Eq. (3) may be separated into two independent parts by a suitable canonical transformation, which mixes the spin waves on the up-sublattices l and l', and down sublattices m and m', respectively,

$$\begin{aligned} & a_{\vec{k}} = 2^{-1/2}(p_{\vec{k}} + q_{\vec{k}}) , \quad c_{\vec{k}} = 2^{-1/2}(p_{\vec{k}} - q_{\vec{k}}) , \\ & b_{\vec{k}} = 2^{-1/2}(r_{\vec{k}} + s_{\vec{k}}) , \quad d_{\vec{k}} = 2^{-1/2}(r_{\vec{k}} - s_{\vec{k}}) . \end{aligned} \tag{5}$$

Equation (3) then reduces to

$$\begin{aligned}\mathcal{H} = {} & C + \sum_{\vec{k}} [(g\mu_B H_A + 5|J|S)(p_{\vec{k}}^\dagger p_{\vec{k}} + r_{\vec{k}}^\dagger r_{\vec{k}}) \\ & + 5|J|S\gamma'_{\vec{k}} (p_{\vec{k}} r_{\vec{k}} + p_{\vec{k}}^\dagger r_{\vec{k}}^\dagger)] \\ & + \sum_{\vec{k}} [(g\mu_B H_A + 5|J|S)(q_{\vec{k}}^\dagger q_{\vec{k}} + s_{\vec{k}}^\dagger s_{\vec{k}}) \\ & + 5|J|S\gamma''_{\vec{k}} (q_{\vec{k}} s_{\vec{k}} + q_{\vec{k}}^\dagger s_{\vec{k}}^\dagger)] ,\end{aligned} \tag{6}$$

with

$$\gamma'_{\vec{k}} = \tfrac{1}{5}(4\gamma_{\vec{k}} + 1) , \quad \gamma''_{\vec{k}} = \tfrac{1}{5}(4\gamma_{\vec{k}} - 1) . \tag{7}$$

Both parts may be diagonalized by a standard 2×2 Bogolyubov transformation,[13] thereby going over to new magnon variables $\alpha_{\vec{k}}$, etc. Introducing the anisotropy parameter $\alpha = g\mu_B H_A / 5|J|S$ and the occupation number operators $n_{\vec{k}}^{(1)} = \alpha_{\vec{k}}^\dagger \alpha_{\vec{k}}$, etc., for these magnons, we finally find for the Hamiltonian to lowest order (simple spin-wave theory)

$$\begin{aligned}\mathcal{H} = {} & C' + 5|J_s|S \sum_{\vec{k}} (D_s^2 - \gamma_{\vec{k}}'^2)^{1/2} (n_{\vec{k}}^{(1)} + n_{\vec{k}}^{(2)} + 1) \\ & + 5|J_s|S \sum_{\vec{k}} (D_s^2 - \gamma_{\vec{k}}''^2)^{1/2} (n_{\vec{k}}^{(3)} + n_{\vec{k}}^{(4)} + 1) ,\end{aligned} \tag{8}$$

with $C' = -10|J|N_0 S(S+1) - 2g\mu_B N_0 (2S+1) H_A$, and where we have labeled the exchange constant J and

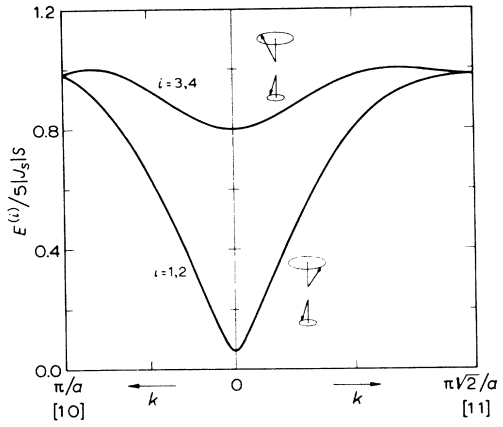

FIG. 2. Dispersion of the 2×2 degenerate spin waves in $K_3Mn_2F_7$ along the [10] and [11] directions in the 2D Brillouin zone. The lower and upper branches correspond to in-phase and out-of-phase precession of the spins in the paired layers, respectively, as indicated schematically. The curves are computed from *un*renormalized theory, with $\alpha_s = 1.9\times10^{-3}$. To convert to renormalized theory, see Eqs. (21a) and (21b).

the anisotropy $D = 1+\alpha$ with the subscript s.

The result is two sets of twofold-degenerate spin-wave branches (Fig. 2), each of which can be split further by an external magnetic field. The energy of the lower branches (1) and (2) increases from the gap energy $E_G = 5|J_s|S(2\alpha_s+\alpha_s^2)^{1/2}$ for the $k=0$ magnon up to $5|J_s|S[(1+\alpha_s)^2-(\frac{1}{5})^2]^{1/2}\approx 0.98\times5|J_s|S$ at the Brillouin-zone boundary. A detailed examination of the transformations involved in the derivation of Eq. (8) reveals that in the semiclassical picture the $k=0$ mode of the lower branch corresponds to a uniform precession of the four sublattices with the sublattices in phase with each other, closely resembling the semiclassical picture of a two-sublattice antiferromagnet.[14] On the other hand, the $k=0$ mode of the upper branches (3) and (4) corresponds to a uniform precession with the sublattices in one layer out of phase with respect to the sublattices in the other layer. The branches (3) and (4) have a $k=0$ energy gap of $5|J_s|S[(\frac{4}{5})^2+2\alpha_s+\alpha_s^2]^{1/2}\approx 0.80\times5|J_s|S$, almost exclusively determined by exchange. Having a rather flat dispersion, they coincide at the zone boundary with the lower branches. Their maximum magnon energy of $5|J_s|S(1+\alpha_s)$, slightly above the zone-boundary value, lies on a contour in the Brillouin zone given by $\cos(\frac{1}{2}k_x a)\cos(\frac{1}{2}k_y a)=\frac{1}{4}$.

One objective of the present study is to determine what improvement can be achieved in describing the sublattice magnetization with spin-wave theory by inclusion of renormalization. Collecting, following Oguchi,[12] all terms in the Hamiltonian up to first order in $1/2S$, we may write the dispersion relation in a form similar to the one given in Ref. 4 for the 2D single-layer structures. That is,

$$E_{\vec{k}}^{(1,2)}/5|J|S = (D^2-\gamma_{\vec{k}}'^2)^{1/2} - g_{\vec{k}}'[R_0+R_1(T)] - \tfrac{1}{4}f_{\vec{k}}'[P_0+P_1(T)], \tag{9a}$$

$$E_{\vec{k}}^{(3,4)}/5|J|S = (D^2-\gamma_{\vec{k}}''^2)^{1/2} - g_{\vec{k}}''[R_0+R_1(T)] - \tfrac{1}{4}f_{\vec{k}}''[P_0+P_1(T)]. \tag{9b}$$

Here we have introduced the quantities

$$g_{\vec{k}}' = (D-\gamma_{\vec{k}}'^2)/(D^2-\gamma_{\vec{k}}'^2)^{1/2}, \qquad g_{\vec{k}}'' = (D-\gamma_{\vec{k}}''^2)/(D^2-\gamma_{\vec{k}}''^2)^{1/2}, \tag{10}$$

$$f_{\vec{k}}' = (\gamma_{\vec{k}}'-1)\gamma_{\vec{k}}'/(D^2-\gamma_{\vec{k}}'^2)^{1/2}, \qquad f_{\vec{k}}'' = (\gamma_{\vec{k}}''+1)\gamma_{\vec{k}}''/(D^2-\gamma_{\vec{k}}''^2)^{1/2}, \tag{11}$$

which contain the $\vec{k}$ dependence of the renormalization. The temperature-independent renormalization is determined by the summations over the Brillouin zone

$$R_0 = \frac{1}{4N_0S}\sum_{\vec{k}}[(g_{\vec{k}}'-1)+(g_{\vec{k}}''-1)], \tag{12}$$

$$P_0 = \frac{1}{4N_0S}\sum_{\vec{k}}(f_{\vec{k}}'+f_{\vec{k}}''), \tag{13}$$

and the temperature-dependent part by

$$R_1(T) = \frac{1}{4N_0S}\sum_{\vec{k}}[g_{\vec{k}}'(n_{\vec{k}}^{(1)}+n_{\vec{k}}^{(2)})+g_{\vec{k}}''(n_{\vec{k}}^{(3)}+n_{\vec{k}}^{(4)})], \tag{14}$$

$$P_1(T) = \frac{1}{4N_0S}\sum_{\vec{k}}[f_{\vec{k}}'(n_{\vec{k}}^{(1)}+n_{\vec{k}}^{(2)})+f_{\vec{k}}''(n_{\vec{k}}^{(3)}+n_{\vec{k}}^{(4)})]. \tag{15}$$

The terms in Eq. (9) with P_0 and $P_1(T)$, which have no analog in the renormalized dispersion relation of the single-layer structures, originate from the fivefold coordination of the magnetic sites rather than a fourfold one with inversion. Finally, the occupation numbers $n_{\vec{k}}^{(i)}$ occurring in $R_1(T)$ and $P_1(T)$ are equated to the Bose factors

$$n_{\vec{k}}^{(i)} = [\exp(E_{\vec{k}}^{(i)}/k_BT)-1]^{-1}, \tag{16}$$

thus making the dispersion relation Eqs. (9a) and (9b) self-consistent.

The sublattice magnetization is given by $M(T) = N_0 g\mu_B\langle S^z\rangle$ with

$$\langle S^z\rangle = S-\Delta_0-\Delta S(T). \tag{17}$$

Here, Δ_0 is the zero-point spin reduction, given by

$$\Delta_0=\frac{1}{4N_0}\sum_{\vec{k}}\left[\left(\frac{D}{(D^2-\gamma_{\vec{k}}'^2)^{1/2}}-1\right)+\left(\frac{D}{(D^2-\gamma_{\vec{k}}''^2)^{1/2}}-1\right)\right], \tag{18}$$

while the temperature-dependent part of $\langle S^z\rangle$ can be expressed as

$$\Delta S(T)=\frac{1}{4N_0}\sum_{\vec{k}}\left(\frac{D}{(D^2-\gamma_{\vec{k}}'^2)^{1/2}}(n_{\vec{k}}^{(1)}+n_{\vec{k}}^{(2)})+\frac{D}{(D^2-\gamma_{\vec{k}}''^2)^{1/2}}(n_{\vec{k}}^{(3)}+n_{\vec{k}}^{(4)})\right). \tag{19}$$

It is noteworthy that for very low temperatures the decrement of the magnetization $\Delta S(T)$ can be expressed in an approximative analytic form. Substituting in Eqs. (8) and (19) the k^2 approximation $\gamma_{\vec{k}}'^2=1-\frac{1}{5}a^2k^2$, neglecting terms with $n_{\vec{k}}^{(3)}$ and $n_{\vec{k}}^{(4)}$, and extending the upper limits of the integrals to infinity, one finds

$$\Delta S(T)=-[(1+\alpha_s)k_BT/4\pi|J_s|S]\ln(1-e^{-T_G/T}), \tag{20}$$

with $T_G=E_{k=0}^{(1,2)}/k_B$, which is precisely one half of the result for the 2D single-layer lattice.[15] This indicates that the functional dependence of $\Delta S(T)$ in the double layer very nearly resembles $\Delta S(T)$ in the single-layer structures, at least up to T_G.

As discussed previously,[4] at low temperatures the effects of renormalization are nearly invisible when measuring thermodynamic quantities. However, renormalization does change the parameters in the dispersion relation deduced from such measurements. In other words, at *low* temperatures the dispersion may equally well be represented by the simple spin-wave dispersion Eq. (8), but with *effective* values J_s and α_s for the exchange constant J and the anisotropy parameter α. Equating, slightly arbitrarily, the lower-branch part of Eq. (8) and Eq. (9a) at the zone center and at the zone boundary, we find for vanishing α, $R_1(T)$, and $P_1(T)$,

$$J_s=J(1-R_0-\tfrac{1}{24}P_0), \tag{21a}$$

$$\alpha_s=\alpha/(1-R_0-\tfrac{1}{12}P_0), \tag{21b}$$

which may be approximated further to $J_s\approx J(1-R_0)$ and $\alpha_s\approx\alpha/(1-R_0)$, as is seen from the actual values R_0 and P_0 to be discussed below. In Sec. III the improvement in the adjustment of theory to experiment by temperature-dependent renormalization R_1 will be compared to the results of a calculation using the unrenormalized energies with the effective parameters.

It is an unfortunate but experimentally well established fact that the decrease of the spin-wave energy gap $E_{k=0}^{(1,2)}$ with temperature is only partly described by the temperature-dependent renormalization arising from terms of order $1/2S$ in the Hamiltonian. To include the additional temperature-dependent renormalization we have adopted $E_{k=0}^{(1,2)}$, or rather the anisotropy parameter α, to vary with temperature in a semiempirical way. It is known from antiferromagnetic resonance that in the single-layer compounds K_2MnF_4,[16] and K_2NiF_4,[17] the gap $E_{k=0}^{(1,2)}$ scales with the sublattice magnetization. We assume the same to be the case in $K_3Mn_2F_7$, i.e., $\alpha(T)$ is determined by solving the equation [cf. Eq. (9a) for $k=0$]

$$E_{k=0}^{(1,2)}(T)=E_{k=0}^{(1,2)}(0)[M(T)/M(0)]=5|J|S\left((2\alpha+\alpha^2)^{1/2}-\frac{[R_0+R_1(T)]\alpha}{(2\alpha+\alpha^2)^{1/2}}\right). \tag{22}$$

It is noted that this relation very nearly corresponds to $\alpha(T)=\alpha(0)[M(T)/M(0)]^2$, which has been derived earlier for a tetragonal lattice.[18,19] The two relations were found not to lead to appreciably different results.

In the computer evaluation of the dispersion relation and the subsequent calculation of $\langle S^z\rangle$, the self-consistency implied by Eq. (16) is implemented by an iterative process. At a certain temperature, given an initial choice for α, first R_0 and P_0 are calculated by the summations [Eqs. (12) and (13)] over the Brillouin zone. Then, the set of Eqs. (9)–(11) and (14)–(16) are iterated to obtain the remaining constants of the dispersion relation Eq. (19), $R_1(T)$ and $P_1(T)$. Finally, Eq. (22) is used to determine a new α, and the iterative process is repeated, if necessary. It is noted at this point that the evaluation of the summations over the Brillouin zone was done without approximations by making use of the identity

$$N_0^{-1}\sum_{\vec{k}}F(\gamma_{\vec{k}})=\frac{4}{\pi^2}\int_0^1 dz\,K((1-z^2)^{1/2})F(z), \tag{23}$$

where for $K(m)=\int_0^{\pi/2}d\phi\,(1-m^2\sin^2\phi)^{-1/2}$, a complete elliptic integral of the first kind, fast computer routines are available.

With respect to actual contributions of P_0 and $P_1(T)$ to the dispersion in $K_3Mn_2F_7$, it turns out that for the low-lying branches (1) and (2) they are smaller than the contributions of R_0 and $R_1(T)$ by at least an order of magnitude. For the appropriate $\alpha=0.00198$, $R_0=-0.0244$, and $P_0=-0.0022$, only weakly dependent on α. Their prefactors in Eq. (9a) are $g_{\vec{k}}'=\alpha/(2\alpha+\alpha^2)^{1/2}\approx 0.03$ and $f_{\vec{k}}'=0$ at $k=0$, while $g_{\vec{k}}'\approx 1$ and $\frac{1}{4}f_{\vec{k}}'\approx -0.04$ at the zone boundary. Similar conclusions hold for the effects of $P_1(T)$ relative to $R_1(T)$, as is observed from Fig. 3. In fact, nowhere in the Brillouin zone does the correction to the spin-wave energy due to P_0

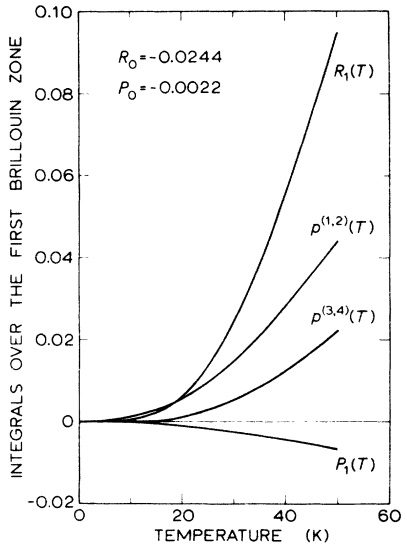

FIG. 3. Integrals over the first Brillouin zone occurring in spin-wave theory vs the temperature. The temperature-dependent renormalization is reflected in $R_1(T)$ and $P_1(T)$, while $p^{(1,2)}(T)$ and $p^{(3,4)}(T)$ are the averaged occupations (*not* including the factor 2 of the degeneracy) of the lower and upper spin-wave branches, respectively. The temperature-independent renormalizations R_0 and P_0 are virtually constant, and are given as figure entries. The integrals have been computed during the iterative process to yield $\langle S^z(T)\rangle$, as described in text, with $J/k_B=-7.59$ K and $\alpha(0)=1.98\times10^{-3}$.

and $P_1(T)$ exceed one tenth of a percent, and their effects appear to be almost unnoticeable in the following calculations. It is further noted here that the temperature-dependent renormalization $R_1(T)$ of the magnon energies is opposite to the renormalization at zero temperature R_0. Finally, Fig. 3 shows the average occupation number over the zone (divided by $4S$),

$$p^{(i)}=\frac{1}{4N_0S}\sum_{\vec{k}} n_{\vec{k}}^{(i)}, \tag{24}$$

again obtained during the iterative process just described. It is observed that above, say, 20 K the upper branch (3, 4) is significantly populated relative to the lower one (1, 2) and therefore may not be omitted in calculating magnetic properties from spin-wave theory. For example, the contribution of the upper branch to $\Delta S(T)$, Eq. (19), is ~5% at 20 K.

III. EXPERIMENTAL

Crystals of $K_3Mn_2F_7$ of typical size 10 mm^3 have been grown from the melt with the horizontal-zone-melting technique. It is difficult to distinguish $K_3Mn_2F_7$ from K_2MnF_4 macroscopically because of the similarity of crystal structure and pink color. The dimensions of the tetragonal crystallographic unit cell have been published by Cousseins[20] to be $a_0=a/\sqrt{2}=4.19$ Å, $c_0=21.66$ Å at room temperature. However, these values are possibly less accurate, since the same values for a_0 were reported in $KMnF_3$ and K_2MnF_4. Because an accurate knowledge of this parameter provides an estimate of the exchange constant, we redetermined the lattice constants of $K_3Mn_2F_7$ at room temperature. The results are $a_0=4.191\pm0.005$ Å and $c_0=21.62\pm0.03$ Å. Recent values by Navarro *et al.*[9] are $a_0=4.183\pm0.002$ Å and $c_0=21.592\pm0.008$ Å.

The temperature dependence of the sublattice magnetization has been measured by observing the NMR frequency $f(T)$ of ^{19}F nuclei adjacent to Mn^{2+} ions in the double layer. In zero external magnetic field these nuclei resonate in a transferred hyperfine field, partly of dipolar origin (~25%) and scaling with the sublattice magnetization as expressed by $f(T)=A(^{19}F)\langle S^z\rangle/h$, where $A(^{19}F)$ is the transferred hyperfine coupling constant. The NMR frequency was measured by exciting the nuclei with a high-power rf pulse with a duration of a few μsec, and beating the free-induction decay following the excitation with a standard oscillator. The coil wound around the sample was used for both excitation and detection. The external field being zero, the orientation of the sample is essential only with respect to the rf field, which should be perpendicular to the tetragonal axis. The detection system consisted of a tunable very-high-frequency receiver with fast recovery against overload, followed by a balanced mixer driven by the standard oscillator. The decay times were of the order of 10 μsec at 4.2 K, decreasing slightly at higher temperatures. At low temperatures the width of the NMR amounted to 40 kHz, apparently of inhomogeneous origin and probably due to local distortions of the magnetic lattice, increasing to about 200 kHz at 35 K. The relaxation time T_1 was about $\frac{1}{2}$ min at 1.5 K, a few seconds at 4.2 K, dropping to a few milliseconds as soon as the temperature was raised above the magnon energy gap.

Temperature stabilization below 4.2 K was accomplished by controlled pumping of the liquid helium in which the sample was immersed, above 4.2 K by controlled heating of a continuous helium gas stream with a stability of 0.02 K. Temperatures were measured with a germanium resistor, carefully calibrated against standard platinum and germanium resistors, with an estimated inaccuracy of 15 mK below 4.2 K and 50 mK at the higher temperatures. In the following analysis (Sec. IV) the inaccuracy in the temperature, which is the major source of the experimental uncertainties,

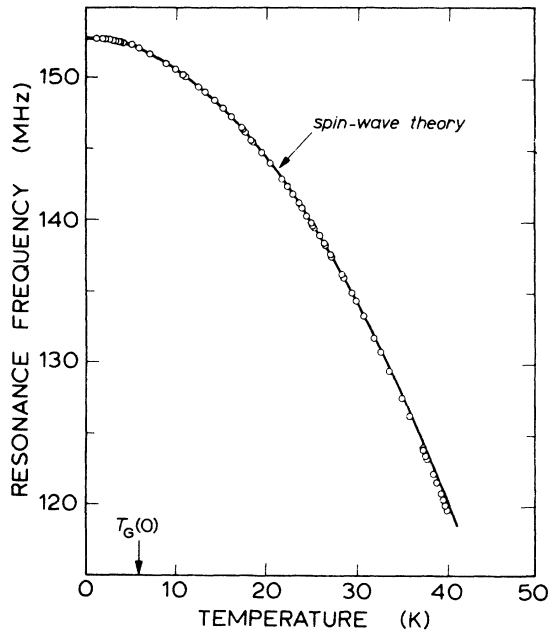

FIG. 4. NMR frequency $f(T)$ of the ^{19}F nuclei adjacent to the magnetic double layer vs temperature. The spin-wave energy gap is indicated by $T_G(0)$. The solid curve is calculated from a least-squares adjustment to renormalized spin-wave theory.

has been propagated to the error in the frequency. The overall inaccuracy of the frequency then is five parts in 10^5 at the lowest temperatures, increasing to five parts in 10^4 at 30 K. The experimental results are presented in Fig. 4, where it is noted that the accuracy cannot be represented on the scale of the figure.[21]

IV. DISCUSSION

In this section, we will present the results of a least-squares analysis of the experimental data in terms of the spin-wave results for the sublattice magnetization and the zero-point spin reduction with inclusion of Oguchi-type renormalization, as obtained in Sec. II. In addition, we will discuss the temperature dependence of the sublattice magnetization of the double layer in comparison to the single layer as well as the 3D antiferromagnet.

In the least-squares fit three adjustable parameters have been used, viz., the exchange constant J, the gap $T_G(0)$ of the spin-wave spectrum at $T = 0$ K, and the zero-temperature NMR frequency $f(0)$. Here it is already noted that $f(0)$ is determined to high precision, and turns out to be only very weakly correlated to the least-squares output values for J and $T_G(0)$. Therefore, we will not consider $f(0)$ further in connection with the least-squares fit, and quote its value as a figure entry only (Fig. 5). To find the largest temperature region of concurrence between theory and experiment, within the experimental errors, we have extended the temperature range of the least-squares adjustment from the data points at the lowest temperature (1.2 K) to a series of different upper temperature limits. In Fig. 5 the results of the fits are given in a condensed form. The errors in the least-squares output values of the parameters, propagated from the errors in the NMR frequencies, are adopted to be twice the standard deviations, corresponding to a 98% probability of finding the true values within the errors. The output values for J and $T_G(0)$ are however strongly correlated. For two upper limits of the temperature we have plotted error ellipses corresponding to two standard deviations, i.e., contours enclosing the 98% probability area of a particular *combination* of J and $T_G(0)$, to show the strong decrease in error limits when the fitting range is extended to higher temperatures, while for the other upper temperatures only the centers of the ellipses are given. Due to the high correlation (the correlation coefficient σ is about -0.98 for all fits), these points are scattered roughly along a straight line. Above 28 K there is, however, a distinct trend for the centers to move downwards. Beyond this temperature the area of the error ellipses starts to

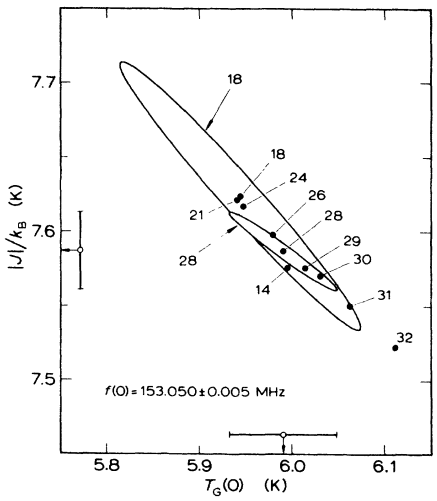

FIG. 5. Output values of the least-squares adjustments of the NMR frequency $f(T)$ in $K_3Mn_2F_7$ to renormalized spin-wave theory. The closed circles represent the output values for the exchange J and the zero-temperature gap $T_G(0)$ obtained from fits to all data up to the temperatures indicated. Error ellipses of two standard deviations are given for the fits up to 18 and 28 K only. The projections of the 28 K ellipse on the axes represent the most accurate values for J and $T_G(0)$.

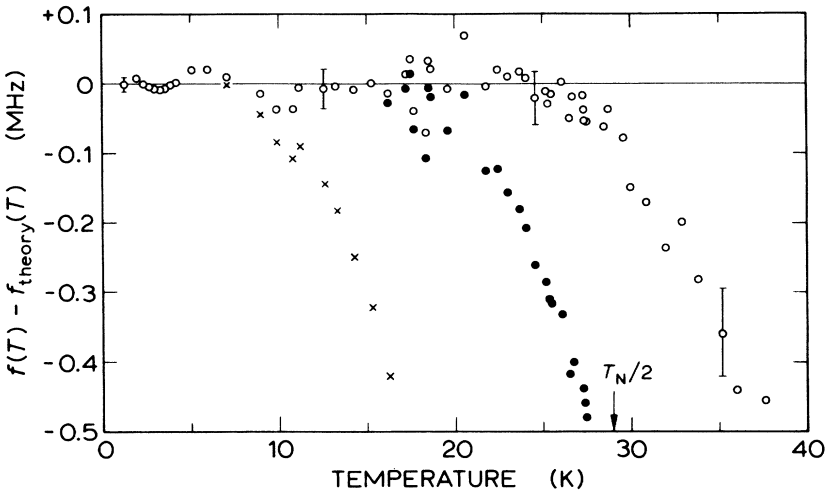

FIG. 6. Deviation of the experimental resonance frequency $f(T)$ in $K_3Mn_2F_7$ from the frequency calculated from renormalized spin-wave theory (open circles) with the parameters obtained in the least-squares fit up to 28 K. Note the distinct break from renormalized theory above this temperature. The result of *un*renormalized theory (closed circles), with effective parameters J_s and α_s [see Eqs. (21a) and (21b)] derived from the renormalized fit up to 28 K, shows that renormalization extends the range of concurrence by 9 K. The result of spin-wave theory in the k^2 approximation (crosses), with J_s and α_s as for the unrenormalized theory, indicates the necessity of integrating exactly over the Brillouin zone.

increase, and it appears to be no longer feasible to fit theory to the data within the experimental errors. In summary, it is believed that the upper limit of 28 K represents the onset of the breakdown from spin-wave theory with the inclusion of the Oguchi corrections. The fit up to 28 K then is the most accurate one, the output values of which are the exchange constant $J/k_B = -7.59 \pm 0.03$ K and the zero-temperature gap $T_G(0) = 5.99 \pm 0.06$ K. With these values the solid line in Fig. 4 is calculated. To demonstrate the breakdown of spin-wave theory more clearly, we also plotted the deviation between experimental and calculated NMR frequencies $f(T) - f_{\text{theor}}(T)$ against the temperature in Fig. 6 as the open circles. To show the improvement that could be obtained by including the temperature-dependent Oguchi corrections $R_1(T)$ and $P_1(T)$ in the dispersion relation, in Fig. 6, the results are included as the dotted points, of a calculation based on simple spin-wave theory [Eq. (8)], but with effective parameters J_s and α_s as explained in Sec. II. While below 18 K there is no significant difference between the two calculations, the onset of the breakdown is reduced by 9 K. The crosses in Fig. 6 again represent simple spin-wave theory, but with the dispersion relation in the k^2 approximation [see Eq. (20)]. The beginning of the breakdown is dramatically reduced to 8 K, indicating that it is essential to carry out the summations over the Brillouin zone exactly.

Further inspection of the calculations reveals that the contribution from the upper-magnon dispersion branches (3) and (4) already becomes of importance beyond 12 K, at a point where the occupation numbers $n_{\vec{k}}^{(3,4)}$ are still less than, say, 2×10^{-3}. This is due to the flat dispersion of the upper magnon branches, so that, although a particular mode contributes only little to the decrement of the magnetization, the collective contribution from all modes over the Brillouin zone results in a noticeable effect (cf. Fig. 3).

In Secs. IV A–IV E we will successively discuss in detail the output values of the least-squares adjustment and some parameters deduced from them.

A. Exchange constant

We first compare the present output value for the exchange J with some recent experimental values. At low temperatures, two-magnon Raman scattering,[22] in which magnons near the Brillouin-zone boundary are observed rather than those in the center of the zone, yielded $J/k_B = -7.54 \pm 0.12$ K, in excellent agreement with the value obtained here. Excellent accord is also found with the exchange parameter determined by us from the susceptibility of a single-crystal specimen.[10] From spin-wave theory applied to the perpendicular susceptibility at zero temperature, $J/k_B = -7.62 \pm 0.15$ has been obtained, while a spin-wave analysis of the parallel susceptibility as a function of tempera-

ture yielded $J/k_B = -7.7 \pm 0.2$ K. At temperatures *above* the Néel point, Navarro *et al.*,[9] using a high-temperature series for the susceptibility of n-layer Heisenberg films,[8] derived from the susceptibility of a powdered sample a value of $J/k_B = -8.08 \pm 0.32$ K, definitely beyond the error limits with respect to the result below T_N. We have also carried out susceptibility measurements on the single crystal in the paramagnetic regime.[10] Full agreement with their conclusions was found ($J/k_B = -8.04 \pm 0.24$ K), but it is noted that also our single crystal data did not fit the series expansion correctly in the region of maximum susceptibility just above T_N. The latter point leads one to the tentative observation that J values deduced from the series expansion may exhibit a systematic error. Another possibility is the occurrence of a crystallographic phase transition around T_N, which would slightly change the interaction distances. In fact our measured susceptibility perpendicular to the c axis shows a small oscillation at the transition.

It is of interest to see whether there exists a monotonic variation of the J values with the Mn^{2+}–Mn^{2+} distance in the related manganese compounds $K_3Mn_2F_7$, K_2MnF_4, and $KMnF_3$. The exchange coupling depends strongly on the Mn^{2+}–Mn^{2+} distance a_0, varying between $J \propto a_0^{12}$ and $J \propto a_0^{20}$, as has been found both experimentally and theoretically.[23,24] When for a_0 in $K_3Mn_2F_7$ the average of the values quoted in Sec. III is taken, we have $a_0 = 4.188$ Å at room temperature. For K_2MnF_4 and $KMnF_3$ these distances are, on the average,[23] $a_0 = 4.172$ Å and $a_0 = 4.190$ Å, respectively. This suggests a conformity between the exchange coupling in $K_3Mn_2F_7$ and $KMnF_3$, which is confirmed by the experimental value for the latter at low temperatures $J/k_B = -7.6 \pm 0.2$ K.[25]

We have also considered the possibility of a difference between the Mn^{2+} – Mn^{2+} exchange constant along the c axis and the exchange constant within the layer, as a result of small differences in the corresponding Mn^{2+}–Mn^{2+} distances. However, from analysis of the sublattice data it appears impossible to resolve such a difference in the exchange within (J) and between (J') the paired layers. Least-squares adjustment of the properly modified Eqs. (9)–(19) with the two J's differing by say 10% still extends to the same limiting temperature of 28 K, but with somewhat modified least-squares output parameters for J and $T_G(0)$. We limit the discussion to an example to show the influence on the fitted parameters. With $J' = 0.9J$ (corresponding to an elongation of about 0.03 Å along the c axis, which may be considered to be an upper limit) we find for the intralayer exchange $J/k_B = -7.70 \pm 0.03$ K and for the zero-temperature gap $T_G(0) = 5.87 \pm 0.06$ K. Numerically, it appeared that the exchange constant weighted by the number of neighbors, i.e., $\frac{1}{5}(4J + J')$ stays nearly constant, while the fitted gap scales with $(4J + J')/5J$.

B. Zero-temperature energy gap

From the energy gap at $T = 0$ K [cf. Eq. (9a)] we derive for the anisotropy constant $\alpha(0) = (1.98 \pm 0.06) \times 10^{-3}$, which corresponds to a staggered anisotropy field $H_A = 1.40 \pm 0.04$ kG. Lattice summation with $\langle S^z \rangle = 2.376$, i.e., with inclusion of the zero-point spin reduction (see below), yields for the dipolar field $H_D = 1.20$ kG, which corroborates the notion that the anisotropy field is mainly of dipolar origin. The difference of 0.2 kG must be attributed to crystalline-field effects, where it is noted that the difference is of the same size, but of opposite sign, as in the single-layer K_2MnF_4. Further it is noted that the gap at $T = 0$ K corresponds to a spin-flop field of 44.6 ± 0.5 kG.

It should be emphasized, however, that the present results for gap and spin-flop field are susceptible to the effects of residual exchange J_c with magnetic ions in next-nearest double layers. Such an exchange coupling along the c axis can be represented by an effective energy gap[4] $E_{k=0}^{\text{eff}} \approx E_{k=0}(1 + |J_c|/5|J|\alpha)$, where $E_{k=0}^{\text{eff}}$ is the gap measured on the basis of the least-squares adjustment used here, and $E_{k=0}$ is the real gap, which is *smaller* for both ferromagnetic and antiferromagnetic J_c. The consequence is that J_c as small as $|J_c/J| \approx 10^{-4}$ will result in deviations outside the error limits between the gap as deduced from the sublattice magnetization and experiments in which the energy gap is measured directly, such as antiferromagnetic resonance. Further conclusions await such measurements to be done.

C. Zero-point spin reduction

A quantity in which the dimensionality of the magnetic lattice is strongly reflected is the zero-point spin reduction. Because the anisotropy field favors the complete alignment of the spins, the reduction Δ_0 is dependent on α, and in fact Δ_0 is vanishingly small for $\alpha \to \infty$. Since the density of magnon states of long wavelengths, which give the main contribution to Δ_0 [Eq. (18)], is higher the lower the dimensionality of the lattice, the reduction is strongly raised when the dimensionality is lowered. In the absence of anisotropy, spin-wave theory yields for the 2D simple-quadratic lattice $\Delta_0 = 0.197$, for the double layer $\Delta_0 = 0.136$, and for the 3D simple-cubic (sc) lattice $\Delta_0 = 0.078$.

Experimentally, the zero-point spin reduction can be determined via the hyperfine field exerted on the nucleus of the magnetic ion itself, or the nucleus of a surrounding ion. Because of the un-

certainties in the hyperfine coupling constant, the reduction in 3D is only marginally resolved (MnF_2: $\Delta_0 = 0.0043 \pm 0.0034$).[26] In the compound K_2MnF_4, where the effect is more pronounced, good accord has been found between experiment, $\Delta_0 = 0.17 \pm 0.03$,[27] and the spin-wave result with inclusion of $\alpha = 0.0038$, $\Delta_0 = 0.170$.

For the double layer $K_3Mn_2F_7$, an estimate of the zero-point spin reduction was made by comparing the zero-temperature NMR frequencies of $K_3Mn_2F_7$ and K_2MnF_4. The transferred hyperfine coupling constant $A(^{19}F)$ has been assumed the same for both compounds, but a correction for a different dipolar lattice contribution has been incorporated. With these assumptions for the zero-point spin reduction $\Delta_0 = 0.12 \pm 0.03$ is deduced. Spin-wave theory with inclusion of anisotropy [Eq. (18)] yields $\Delta_0 = 0.124$, where it is noteworthy that the contribution of the upper branches (3) and (4) amounts to 0.011. The agreement is perhaps somewhat fortuitous considering the uncertainties in the coupling constant $A(^{19}F)$ in $K_3Mn_2F_7$, but anyway the result indicates that the zero-point spin reduction is intermediate between the 2D and 3D sc lattices.

D. Néel temperature

It is not feasible to obtain an accurate value of the Néel temperature by extrapolating the NMR data to zero frequency because of the increase of the linewidth in approaching the transition and the small size of the crystal. We found $T_N = 60 \pm 5$ K from comparison with K_2MnF_4, while in recent susceptibility measurements[10] we arrived at $T_N = 58 \pm 1$ K. In this connection it is noteworthy that Ikeda and Hirakawa[28] reported a second phase transition at 58 K in their neutron experiments on K_2MnF_4, which they attributed to an ordering to a Ca_2MnO_4 magnetic structure. It seems now more likely that some $K_3Mn_2F_7$ was present in their sample. An estimate of the transition temperature can also be made by use of a theoretical result by Ritchie and Fisher,[8] who obtained $T_N = 1.25|J|S^2$ from the analysis of a high-temperature series expansion for n-layer Heisenberg films. Although derived for a ferromagnetic exchange, this yields $T_N = 59.4$ K, a value in reasonable agreement with the above results.

E. Comparison with 2D and 3D

To compare the double-layer antiferromagnet with the 2D quadratic single layer on one hand and the "infinite-layer" 3D sc antiferromagnet on the other hand, we calculated in Fig. 7 the sublattice magnetization versus the temperature for the three structures on the basis of spin-wave theory. Here, the sublattice magnetization is normalized to the fully aligned Néel state, while the temperature is scaled with respect to the relevant parameter in spin-wave theory, the exchange energy $z|J|S$, where z is the number of nearest neighbors. To facilitate comparison we adopted for all structures $S = \frac{5}{2}$ and $\alpha = 0.002$, as appropriate for the double-layer $K_3Mn_2F_7$. For the double layer and the single layer the calculations are "exact", i.e., spin-wave theory was renormalized according to Oguchi, a temperature-dependent anisotropy was used, and the summations were carried out over the complete Brillouin zone without approximations (cf. Sec. II). For the temperature dependence of the sublattice magnetization of the 3D cubic system, an approximative analytic expression originally given by Eisele and Keffer[29] was used, which, although valid for the low-temperature region only, is sufficiently accurate for our present purposes. At temperatures in the neighborhood of the transition temperature, spin-wave theory as used here underestimates the drop in the magnetization, but some idea about the course of the curves to the right may be obtained from the transition points of the three structures, which experimentally are $k_B T_N/z|J|S = 0.50$ for the single layer,[1] 0.61 for the double layer,[10] and 0.80 for the 3D structure.[1]

As was indicated in connection with the analytic expression in the k^2 approximation Eq. (20), the functional dependence of the magnetization at low temperatures is the same for the double layer and the single layer, apart from a constant factor. The reasons for this are, first, that magnons in the upper two branches (3) and (4) are virtually

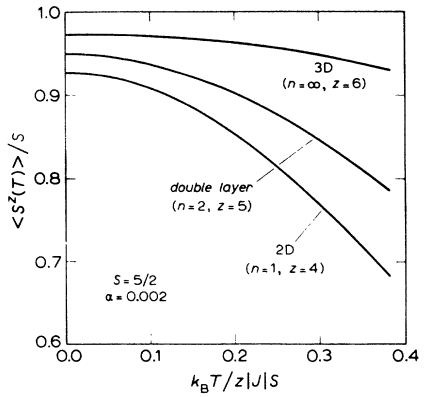

FIG. 7. Sublattice magnetization as a function of the reduced temperature for the simple-quadratic (2D) single layer ($n=1$, $z=4$), the simple-quadratic double layer ($n=2$, $z=5$) and the simple-cubic (3D) lattice ("infinite layer," $n=\infty$, $z=6$). The curves are computed from spin-wave theory, as described in text. To facilitate comparison, for all structures $S=\frac{5}{2}$ and $\alpha=0.002$ has been adopted. Also note the dependence of the zero-point spin reduction on n.

not excited at low temperatures, which as compared to the single layer halves the number of occupied states per magnetic ion, and, secondly, that for low k the dispersion relation for the lower branch reduces to the single layer result, except for a factor $\frac{5}{4}$ due to the different number of magnetic neighbors. Thus at low temperatures the decrement of magnetization of the double layer, with reference to zero temperature, is $\frac{1}{2}\times\frac{5}{4}=0.625$ times that of the single layer. Inspection of Fig. 7 reveals that this factor is rather well preserved also at the higher temperatures, the reason obviously being that even then the low-k region of the Brillouin zone provides the main contribution to the magnetization. A similar conclusion is expected to hold for a three-layer antiferromagnet, which has three twofold-degenerate spin-wave branches, with a smaller factor (~0.5), and so on. However, when increasing the number of layers, the spacing between the spin-wave branches will eventually become smaller than k_BT, so that higher branches, which correspond to $k\neq 0$ along the z axis, will be populated. In other words, the discrete dispersion along the z axis will go over to a continuum, and the functional dependence of the magnetization on temperature will be 3D rather than 2D.

The similarity of the temperature dependence of the sublattice magnetization in the double layer and single layer is also reflected in the experimental fact that renormalization effects in both $K_3Mn_2F_7$ and K_2MnF_4 become visible outside the error limits at temperatures beyond $k_BT/z|J|S\approx 0.20$. Likewise, in both structures spin-wave theory with proper renormalization throughout the entire Brillouin zone appears to break down at a temperature slightly lower than half the transition point. In $K_3Mn_2F_7$ the extension of the fit by renormalization is about 9 K, as compared to 3 K for K_2MnF_4. Still, it is not likely that a different type or higher-order renormalization will substantially improve upon the concurrence of spin-wave theory and experiment. Instead, as was found to be the case in the single layers K_2MnF_4, Rb_2MnF_4, and K_2NiF_4,[4] the point $\frac{1}{2}T_N$, or perhaps a slightly higher temperature in case of the double layer, seems to be a characteristic temperature, where spin deviations not properly treated by spin-wave theory set in.

V. CONCLUSIONS

The main results of this investigation can be summarized as follows. A least-squares adjustment of the experimental data to spin-wave theory with inclusion of Oguchi renormalization to first order in 1/2S as well as temperature-dependent renormalization of the spin-wave gap yields an excellent fit, within the experimental errors, up to 28 K. At this temperature the magnetization has dropped by 11% relative to the zero-temperature value, as compared to 7% at the point of breakdown in the single-layer structure K_2MnF_4. The temperature-dependent renormalization results in a marked improvement of about 9 K in the fit. Also accordance, perhaps slightly fortuitous in view of the experimental method, has been found between the experimental zero-point spin reduction and the relevant spin-wave result. The output parameters of the adjustment, i.e., the exchange constant J, the zero-temperature spin-wave gap $T_G(0)$, and the zero-temperature resonance frequency $f(0)$ have been summarized in Table I. We have also tabulated some derived quantities, such as the anisotropy parameter α, and some spin-wave constants reflecting the dimensionality of the magnetic lattice, such as the temperature-independent renormalizations P_0 and

TABLE I. Summary of various quantities for the double-layer antiferromagnet $K_3Mn_2F_7$, and comparison with the corresponding values of the single-layer K_2MnF_4. Unless indicated otherwise, the values for $K_3Mn_2F_7$ refer to the present work, those for K_2MnF_4 to Ref. 4.

Parameter	$K_3Mn_2F_7$	K_2MnF_4
T_N(K)	58 ± 1 [a]	42.1 [b]
Δ_0	0.124 [c]	0.170 [d]
	0.12 ± 0.03	0.17 ± 0.03 [e]
R_0	−0.0244 [f]	−0.0316
P_0	−0.0022 [g]	...
$f(0)$(MHz)	153.050 ± 0.005	150.477 ± 0.003
J/k_B(K)	-7.59 ± 0.03	-8.41 ± 0.06
	-7.62 ± 0.15 [h]	
J_s/k_B(K)	-7.78 ± 0.03	-8.67 ± 0.06
$T_G(0)$(K)	5.99 ± 0.06 [i]	7.54 ± 0.07 [i]
$\alpha(0)$	0.0020	0.0038
H_A(kG)	1.40	2.35
H_D(kG)	1.20 [j]	2.40 [j]

[a] From susceptibility (Ref. 10).
[b] R. J. Birgeneau, H. J. Guggenheim, and G. Shirane, Phys. Rev. B 8, 304 (1974).
[c] Spin-wave value, Eq. (18), assumed in the fitting procedure.
[d] Spin-wave value (Ref. 4).
[e] Reference 27.
[f] Equation (12).
[g] Equation (13).
[h] From spin-wave fit to perpendicular susceptibility at zero temperature (Ref. 10).
[i] Effective values, including effects of residual c-axis exchange coupling (see Appendix B to Ref. 4). In K_2MnF_4 the antiferromagnetic-resonance value, not including these effects, is 7.40 ± 0.05 K (Ref. 16).
[j] With inclusion of zero-point spin reduction.

R_0 and the zero-point spin reduction Δ_0. For comparison, also the corresponding values for the single layer K_2MnF_4 have been included. The exchange parameter obtained here agrees well with those from the susceptibility in the ordered regime, but the observed difference of 5% with J deduced from susceptibility measurements above T_N is not conclusively explained. It is noted that a zero-point spin reduction Δ_0 different from the spin-wave value used here, would result in a slight variation in the value deduced for J, because in the calculations the quality of the least-squares fits is not appreciably altered when J is correlated to Δ_0 according to $J(S-\Delta_0)$ is constant. However, it is highly improbable that this could modify the output value of J by more than 1%, or remove the discrepancy.

In comparing the double-layer structure to the corresponding 2D and 3D structures, it is concluded that the functional dependence of the sublattice magnetization at low temperatures resembles more closely the single-layer structure. This would indeed be expected, since along the c axis of the double-layer structure only two values of k_z are allowed, viz., $k_z=0$ and $k_z=\pi/a'$. These differ in energy by $\sim 4|J|S$ in the zone center (Fig. 2), so that at low temperatures ($k_BT \ll 4|J|S$) the vast majority of thermally excited spin waves will have $k_z=0$. In other words, a particular spin in the upper layer is precessing in phase with its nearest neighbor in the lower layer. The magnon energy of the lower branches is therefore the same as in the single layer, apart from a factor $\sim\frac{5}{4}$ due to the difference in the number of nearest neighbors (and a different α), resulting in a similar dependence of the sublattice magnetization on temperature, at least at low temperatures. In our experiments, however, the effects of excitation of the upper branch of the spin-wave spectrum become noticeable at temperatures above 12 K. From the above point of view it is not surprising that similarly to the 2D structures K_2MnF_4, Rb_2MnF_4, and K_2NiF_4 spin-wave theory breaks down at a temperature slightly lower than $\frac{1}{2}T_N$. As in these last-mentioned compounds it is believed that at this temperature magnetic excitations not properly described by spin-wave theory set in.

ACKNOWLEDGMENTS

The authors wish to acknowledge useful discussions with M. P. H. Thurlings on the transformations involved in the diagonalization of the Hamiltonian. The work is part of the research program of the "Stichting voor Fundamenteel Onderzoek der Materie (FOM)," and has been made possible by financial support from the "Nederlandse Organisatie voor Zuiver Wetenschappelijk Onderzoek (ZWO)."

[1]For a review, L. J. de Jongh and A. R. Miedema, Adv. Phys. 23, 1 (1974).
[2]D. J. Breed, thesis (University of Amsterdam, 1969) (unpublished); Physica (Utr.) 37, 35 (1967).
[3]R. J. Birgeneau, H. J. Guggenheim, and G. Shirane, Phys. Rev. B 1, 2211 (1970).
[4]H. W. de Wijn, L. R. Walker, and R. E. Walstedt, Phys. Rev. B 8, 285 (1973).
[5]E. Gurewitz, J. Makovsky, and H. Shaked, Phys. Rev. B 14, 2071 (1976).
[6]J. Ferguson, E. R. Krausz, G. B. Robertson, and H. J. Guggenheim, Chem. Phys. Lett. 17, 551 (1972).
[7]R. V. Pisarev, J. Ferreé, R. H. Petit, B. B. Krichevtsov, and P. P. Syrnikov, J. Solid State Phys. 7, 4143 (1974).
[8]D. S. Ritchie and M. E. Fisher, Phys. Rev. B 7, 480 (1973).
[9]R. Navarro, J. J. Smit, L. J. de Jongh, W. J. Crama, and D. J. W. IJdo, Physica B (Utr.) 83, 97 (1976).
[10]A. F. M. Arts, C. M. J. van Uijen, J. A. van Luijk, H. W. de Wijn, and C. J. Beers, Solid State Commun. 21, 13 (1977).
[11]G. G. Low, Proc. Phys. Soc. Lond. 82, 992 (1963).
[12]T. Oguchi, Phys. Rev. 117, 117 (1960).
[13]F. Keffer, in *Encyclopedia of Physics*, edited by S. Flügge (Springer, Berlin, 1966), Vol. XVIII/2.
[14]S. Foner, in *Magnetism*, edited by G. T. Rado and H. Suhl (Academic, New York, 1963), Vol. I, p. 391; S. Geschwind and L. R. Walker, J. Appl. Phys. 30, 163S (1959).
[15]H. W. de Wijn, R. E. Walstedt, L. R. Walker, and H. J. Guggenheim, Phys. Rev. Lett. 24, 832 (1970).
[16]H. W. de Wijn, L. R. Walker, S. Geschwind, and H. J. Guggenheim, Phys. Rev. B 8, 299 (1973).
[17]R. J. Birgeneau, F. DeRosa, and H. J. Guggenheim, Solid State Commun. 8, 13 (1970).
[18]T. Oguchi, Phys. Rev. 111, 1063 (1958).
[19]P. Pincus, Phys. Rev. 113, 769 (1959).
[20]J. C. Cousseins, Rev. Chim. Miner. 1, 573 (1964).
[21]The data can be obtained from the authors in tabular form on request.
[22]A. van der Pol, M. P. H. Thurlings, and H. W. de Wijn (unpublished).
[23]L. J. de Jongh and R. Block, Physica B (Utr.) 79, 568 (1975).
[24]K. N. Shrivastava and V. Jaccarino, Phys. Rev. B 13, 299 (1976).
[25]S. J. Pickart, M. F. Collins, and C. G. Windsor, J. Appl. Phys. 37, 1054 (1966).
[26]E. D. Jones and K. B. Jefferts, Phys. Rev. 135, A1277 (1964).
[27]R. E. Walstedt, H. W. de Wijn, and H. J. Guggenheim, Phys. Rev. Lett. 25, 1119 (1970).
[28]H. Ikeda and K. Hirakawa, J. Phys. Soc. Jpn. 33, 393 (1972).
[29]J. A. Eisele and F. Keffer, Phys. Rev. 96, 929 (1954); R. J. Joenk, *ibid.* 128, 1634 (1962).

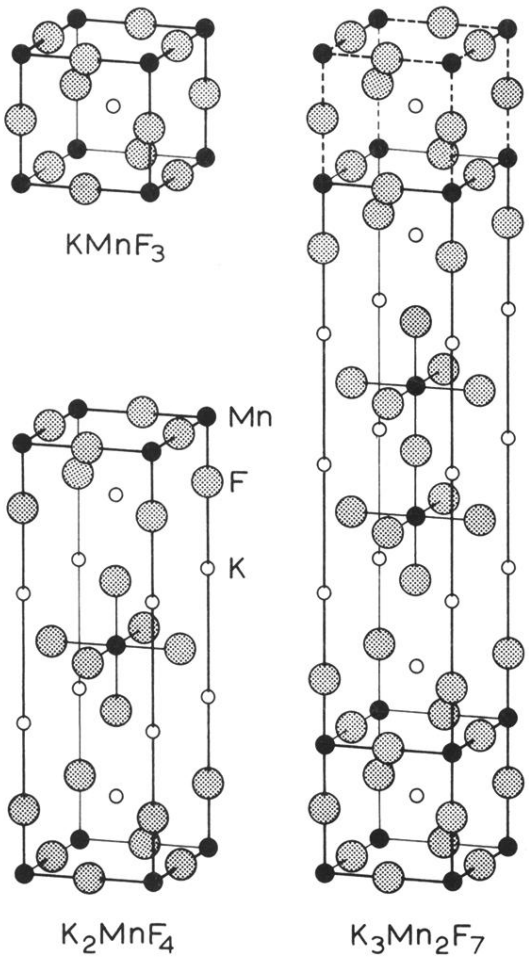

FIG. 1. Crystallographic unit cell of $K_3Mn_2F_7$, as compared to those of $KMnF_3$ and K_2MnF_4. The cell of $K_3Mn_2F_7$ has been extended along the tetragonal axis to indicate more clearly the magnetic double-layer structure.